

An SVD-free Pareto curve approach to rank minimization

Aleksandr Y. Aravkin

*IBM T.J. Watson Research Center
Yorktown Heights, NY 10598, USA*

SARAVKIN@US.IBM.COM

Rajiv Mittal

*Department of Earth and Ocean Sciences, University of British Columbia
Vancouver, BC, Canada*

RAKUMAR@EOS.UBC.CA

Hassan Mansour

*Department of Mathematics and Earth and Ocean Sciences, University of British Columbia
Vancouver, BC, Canada*

HASSANM@CS.UBC.CA

Ben Recht

*Department of Computer Science, University of Wisconsin-Madison
Madison, WI, USA*

BRECHT@CS.WISC.EDU

Felix J. Herrmann

*Department of Earth and Ocean Sciences, University of British Columbia
Vancouver, BC, Canada*

FHERRMANN@EOS.UBC.CA

Editor:

Abstract

Recent SVD-free matrix factorization formulations have enabled rank optimization for extremely large-scale systems (millions of rows and columns). In this paper, we consider rank-regularized formulations that only require a target data-fitting error level, and propose an algorithm for the corresponding problem. We illustrate the advantages of the new approach using the Netflix problem, and use it to obtain high quality results for seismic trace interpolation, a key application in exploration geophysics. We show that factor rank can be easily adjusted as the inversion proceeds, and propose a weighted extension that allows known subspace information to improve the results of matrix completion formulations. Using these methods, we obtain high-quality reconstructions for large scale seismic interpolation problems with real data.

1. Introduction

Sparsity- and rank-regularization have had tremendous impact in many areas over the last several decades. Sparsity in certain transform domains has been exploited to solve underdetermined linear systems with applications to compressed sensing Donoho (2006); Candès & Tao (2006), natural image denoising/inpainting Starck et al. (2005); Mairal et al. (2008); Mansour et al. (2010), and seismic image processing Herrmann & Hennenfent (2008); Neelamani et al. (2010). Analogously, low rank structure has been used to efficiently solve the Netflix problem, along with many other applications Fazel (2002); Recht et al. (2010); Candès et al. (2011).

Regularization formulations for both types of problems introduce a regularization functional of the decision variable, either by adding an explicit penalty to the data-fitting term (QP_λ), or by imposing constraints ($LASSO_\tau$). These approaches require the user to provide regularization pa-

rameters whose values are typically not known ahead of time, and require fitting or cross-validation procedures.

An alternate formulation (BPDN_σ) has been successfully used for the sparse regularization of large scale systems Berg & Friedlander (2008), and proposed for nuclear norm regularization Berg & Friedlander (2011). This formulation requires the user to provide an acceptable error in the data fitting domain (BPDN_σ), and is preferable for many applications, and especially when practitioners know (or are able to estimate) an approximate data error level.

A practical implementation of (BPDN_σ) for large scale matrix completion problems is difficult because of the tremendous size of the systems of interest, which makes SVD-based approaches intractable. Fortunately, a growing literature on factorization-based rank optimization approaches has enabled matrix completion formulations for (QP_λ) and (LASSO_τ) approaches for extremely large-scale systems that avoiding costly SVD computations Rennie & Srebro; Lee et al. (2010); Recht & Ré (2011). In this paper, we extend the framework of Berg & Friedlander (2011) to incorporate matrix factorization ideas, enabling the (BPDN_σ) formulation for rank regularization of extremely large scale problems, such as seismic data interpolation.

The paper proceeds as follows. In section 2, we introduce and compare (QP_λ), (LASSO_τ), and (BPDN_σ). We also review the SPGL_1 algorithm Berg & Friedlander (2008) to solve (BPDN_σ). In section 3, we formulate the convex relaxation for the rank optimization problem, and review SVD-free factorization methods. In section 4, we propose an algorithm that combines matrix factorization with the approach of Berg & Friedlander (2008). We discuss two important extensions to this framework in section 5, and present numerical results for both the Netflix problem and for seismic trace interpolation of real data in section 6.

2. Regularization formulations

There are three main types of regularization formulations, each of which controls the tradeoff between data fitting and a regularization functional using a regularization parameter:

$$\min_x \|\mathcal{A}(x) - b\|_2^2 + \lambda \|x\| \quad (\text{QP}_\lambda)$$

$$\min_x \|\mathcal{A}(x) - b\|_2^2 \quad \text{s.t.} \quad \|x\| \leq \tau \quad (\text{LASSO}_\tau)$$

$$\min_x \|x\| \quad \text{s.t.} \quad \|\mathcal{A}(x) - b\|_2^2 \leq \sigma. \quad (\text{BPDN}_\sigma)$$

In these formulations, x may be either a matrix or a vector, $\|\cdot\|$ may be a sparsity or rank promoting penalty such as $\|\cdot\|_1$ or $\|\cdot\|_*$, and \mathcal{A} may be any linear operator that predicts the observed data vector b .

From an optimization perspective, most algorithms solve (QP_λ) or (LASSO_τ), together with a continuation strategy to modify τ or λ , see e.g., Figueiredo et al. (2007); Berg & Friedlander (2008). However, from a modeling perspective (BPDN_σ) has a significant advantage, since the σ parameter can be directly interpreted as a noise ceiling. In many applications, such as seismic data interpolation, scientists have an (approximate) idea of the noise floor, or a threshold beyond which noise is commensurate with the data.

Berg & Friedlander (2008) proposed the SPGL₁ algorithm for optimizing (BPDN_σ) while working only with (LASSO_τ). Define the *value function*

$$v(\tau) = \min_x \|\mathcal{A}(x) - b\|_2^2 \quad \text{s.t. } \|x\| \leq \tau, \quad (2.1)$$

and then find the root of $v(\tau) = \sigma$ using Newton's method:

$$\tau^{k+1} = \tau^k - \frac{v(\tau) - \sigma}{v'(\tau)}. \quad (2.2)$$

The graph of $v(\tau)$ is often called the Pareto curve. In the context of sparsity optimization, (BPDN_σ) and (LASSO_τ) are known to be equivalent for certain values of parameters τ and σ . Aravkin et al. (2012) extend these results to a very broad class of formulations (see Theorem 2.1)¹.

For the class of problems we consider, it follows from Berg & Friedlander (2011) that $v(\tau)$ is nonincreasing, convex, and differentiable, and

$$v'(\tau) = -\|\mathcal{A}^*(b - \mathcal{A}\bar{x})\|_d, \quad (2.3)$$

where \mathcal{A}^* is the adjoint to the operator \mathcal{A} , $\|\cdot\|_d$ is the dual norm to $\|\cdot\|$, and \bar{x} solves LASSO_τ. Therefore, to design effective optimization methods, one has to be able to evaluate $v(\tau)$, and to compute the dual norm $\|\cdot\|_d$. Evaluating $v(\tau)$ requires solving a sequence of optimization problems (2.1), for the sequence of τ given by (2.2). These problems can be solved inexactly, with increasing accuracy as the optimization proceeds Berg & Friedlander (2008). For large scale systems, the method of choice is typically a first-order method, such as spectral projected gradient. Fast projection is therefore a necessary requirement for tractable implementation, since it is used in every iteration of every subproblem.

Iteration (2.2) converges very fast, so typically only a few (6-10) (LASSO_τ) problems need to be solved to find a solution to (BPDN_σ) for a given σ . As the optimization proceeds, (LASSO_τ) problems for larger τ warm-start from the solution corresponding to the previous τ .

3. Rank optimization

We now consider important details required to implement (BPDN_σ) for rank minimization. We begin by considering the classic approach, with $\|\cdot\|$ taken to be the nuclear norm, where for a matrix $X \in \mathbb{R}^{n \times m}$, $\|X\|_* = \|\sigma_1\|$, where σ is the vector of singular values. The dual norm in this case is σ_∞ , which is relatively easy to find for very large systems.

Much more difficult is solving the optimization problem in (2.1). For the large system case, this would require projecting onto the set $\|X\|_* \leq \tau$, which requires repeated application of SVDs. This is not feasible for large systems.

Factorization-based approaches allow matrix completion for extremely large-scale systems by avoiding costly SVD computations Rennie & Srebro; Lee et al.; Recht & Ré (2011). The main idea is to parametrize the matrix X as a product,

$$X = LR^T, \quad (3.1)$$

1. The hypotheses do not even require convexity of the penalty and regularizer; however, convexity is sufficient for the equivalence result.

and to optimize over the factors L, R . If $X \in \mathbb{R}^{n \times m}$, then $L \in \mathbb{R}^{n \times k}$, and $R \in \mathbb{R}^{m \times k}$. The decision variable therefore has dimension $k(n + m)$, rather than nm ; giving tremendous savings when $k \ll m, n$.

Aside from the considerable savings in the size of the decision variable, the factorization technique gives an additional advantage: it allows the use of a factorization identities to make the projection problem in (LASSO_τ) trivial, entirely avoiding the SVD.

For the nuclear norm, we have Rennie & Srebro

$$\|X\|_* = \inf_{X=LR^T} \frac{1}{2} \left\| \begin{bmatrix} L \\ R \end{bmatrix} \right\|_F^2.$$

Working with a particular representation $X = LR^T$, therefore, guarantees that

$$\|X\|_* = \|LR^T\|_* \leq \frac{1}{2} \left\| \begin{bmatrix} L \\ R \end{bmatrix} \right\|_F^2. \quad (3.2)$$

The nuclear norm is not the only formulation that can be factorized. Lee et al. (2010) have recently introduced the max norm, which is closely related to the nuclear norm and has been successfully used for matrix completion.

4. New algorithm

The factorized formulations in the previous section have been used to design several algorithms for large scale matrix completion and rank minimization Lee et al. (2010); Recht & Ré (2011).

All of these formulations take the form (QP_λ) or (LASSO_τ) , and are optimized using the projected gradient or proximal point algorithms. The disadvantage, just as in analogous formulations for sparsity promotion, is the need to identify parameters λ and τ .

Instead, we propose to solve the (BPDN_σ) formulation using the Pareto approach. We define

$$v(\tau) = \min_X \|\mathcal{A}(X) - b\|_2^2 \quad \text{s.t.} \quad \|X\|_* \leq \tau,$$

and find $v(\tau) = \sigma$ using the iteration (2.2).

However, rather than parameterizing our problem with X , which requires SVDs for the projection, we use the factorization formulation. When evaluating the value function $v(\tau)$, we actually solve

$$\min_{L,R} \|\mathcal{A}(LR^T) - b\|_2^2 \quad \text{s.t.} \quad \frac{1}{2} \left\| \begin{bmatrix} L \\ R \end{bmatrix} \right\|_F^2 \leq \tau. \quad (4.1)$$

By (3.2), any solution $X = LR^T$ is feasible, i.e. $\|X\|_* \leq \tau$. This also holds for any approximate solution. However, it also means that the solutions are conservative, and iteration (2.2) may take more iterations to find the root compared to using the true (but expensive) projection. Adjusting (2.2) to take this into account may further speed up the approach.

The problem (4.1) is optimized using the spectral projected gradient algorithm. The gradient is easy to compute, and the projection requires rescaling all entries of L, R by a single value, which is fast, simple, and parallelizable.

To evaluate $v'(\tau)$, we use the formula (2.3), treating $X = LR^T$ as a matrix in its own right. This requires computing the largest singular value of

$$\mathcal{A}^*(b - \mathcal{A}(\bar{L}\bar{R}^T)) ,$$

which can be done relatively fast.

In section 2, we emphasized the practical advantages of prescribing an error level σ for the (BPDN $_{\sigma}$) formulation. It is important to note that both the SPG ℓ_1 algorithm and the extensions proposed here can be used to get results given a limited computational budget and no σ estimate. Specifically, the algorithm can be initialized with $\sigma = 0$ and run for a fixed number of iterations (to stay within the computational budget). This is exactly what we do for the real-data seismic example in section 6.

5. Further extensions

5.1 Increasing k on the fly

An important aspect to the factorization formulation is the choice of rank for the factors L, R in (3.1). The choice of rank k directly controls the rank of $X = LR^T$, and picking k too small makes it impossible to fit the data up to a target level σ . It is therefore desirable to be able to dynamically increase k , especially for problems with multiscale structure (e.g. seismic data, where k is expected to grow with frequency).

Fortunately, adding columns to L and R can be done on the fly, since

$$\begin{bmatrix} L & l \end{bmatrix} \begin{bmatrix} R & r \end{bmatrix}' = LR^T + lr^T .$$

Moreover, the proposed framework for solving (BPDN $_{\sigma}$) is fully compatible with this strategy, since the underlying root finding is blind to the factorization representation. Changing k only affects iteration (2.2) through $v(\tau)$ and $v'(\tau)$.

5.2 Reweighting

Every rank- k solution \bar{X} of (BPDN $_{\sigma}$) lives in a lower dimensional subspace of $\mathbb{R}^{n \times m}$ spanned by the $n \times k$ row and $m \times k$ column basis vectors corresponding to the nonzero singular values of \bar{X} . In certain situations, it is possible to estimate the row and column subspaces of the matrix X either from prior subspace information or by solving an initial (BPDN $_{\sigma}$) problem.

In the case where X is a vector, it was shown that prior information on the support (nonzero entries) of X can be incorporated in the ℓ_1 -recovery algorithm by solving the weighted- ℓ_1 minimization problem. In this case, the weights are applied such that solutions with large nonzero entries on the support estimate have a lower cost (weighted ℓ_1 norm) than solutions with large nonzeros outside of the support estimate Friedlander et al. (2011).

When X is a matrix, the support estimate is replaced by estimates of the row and column subspace bases $U_0 \in \mathbb{R}^{n \times k}$ and $V_0 \in \mathbb{R}^{m \times k}$ of the largest k singular values of X . Let the matrices $\tilde{U} \in \mathbb{R}^{n \times k}$ and $\tilde{V} \in \mathbb{R}^{m \times k}$ be estimates of U_0 and V_0 , respectively. The weighted nuclear norm minimization problem can then be formulated as follows:

$$\min_X \|QXW\|_* \quad \text{s.t.} \quad \|\mathcal{A}(X) - b\|_2^2 \leq \sigma, \quad (\text{wBPDN}_{\sigma})$$

where $Q = \omega \tilde{U} \tilde{U}' + \tilde{U}^\perp \tilde{U}^{\perp'}$, $W = \omega \tilde{V} \tilde{V}' + \tilde{V}^\perp \tilde{V}^{\perp'}$, and ω is some constant between zero and one. Here, we use the notation $\tilde{U}^\perp \in \mathbb{R}^{n \times n-k}$ to refer to the orthogonal complement of \tilde{U} in $\mathbb{R}^{n \times n}$, and similarly for \tilde{V}^\perp in $\mathbb{R}^{m \times m}$.

A factorization similar to (4.1) can then be formulated for the (wBPDN $_\sigma$) problem in order to optimize over the lower dimensional factors $L \in \mathbb{R}^{n \times k}$ and $R \in \mathbb{R}^{m \times k}$. In particular, we can solve a sequence of (LASSO $_\tau$) problems

$$\min_{L,R} \|\mathcal{A}(LR^T) - b\|_2^2 \quad \text{s.t.} \quad \frac{1}{2} \left\| \begin{bmatrix} QL \\ WR \end{bmatrix} \right\|_F^2 \leq \tau, \quad (5.1)$$

where Q and W are as defined above. Problem (5.1) can also be solved using the spectral projected gradient algorithm. However, unlike to the non-weighted formulation, the projection in this case is nontrivial. Fortunately, the structure of the problem allows us to find an efficient formulation for the projection operator.

5.2.1 PROJECTION ONTO THE WEIGHTED FROBENIUS NORM BALL.

The projection of a point (L, R) onto the weighted Frobenius norm ball $\frac{1}{2} (\|QL\|_F^2 + \|WR\|_F^2) \leq \tau$ is achieved by finding the point (\tilde{L}, \tilde{R}) that solves

$$\min_{\hat{L}, \hat{R}} \frac{1}{2} \left\| \begin{bmatrix} \hat{L} - L \\ \hat{R} - R \end{bmatrix} \right\|_F^2 \quad \text{s.t.} \quad \frac{1}{2} \left\| \begin{bmatrix} Q\hat{L} \\ W\hat{R} \end{bmatrix} \right\|_F^2 \leq \tau.$$

The solution to the above problem is given by

$$\begin{aligned} \tilde{L} &= \left((\mu\omega^2 + 1)^{-1} \tilde{U} \tilde{U}^T + (\mu + 1)^{-1} \tilde{U}^\perp \tilde{U}^{\perp T} \right) L \\ \tilde{R} &= \left((\mu\omega^2 + 1)^{-1} \tilde{V} \tilde{V}^T + (\mu + 1)^{-1} \tilde{V}^\perp \tilde{V}^{\perp T} \right) R, \end{aligned}$$

where μ is the Lagrange multiplier that solves $f(\mu) \leq \tau$ with $f(\mu)$ given by

$$\begin{aligned} \frac{1}{2} \text{Tr} \left[\left(\frac{\omega^2}{(\mu\omega^2 + 1)^2} \tilde{U} \tilde{U}^T + \frac{1}{(\mu + 1)^2} \tilde{U}^\perp \tilde{U}^{\perp T} \right) LL^T \right. \\ \left. + \left(\frac{\omega^2}{(\mu\omega^2 + 1)^2} \tilde{V} \tilde{V}^T + \frac{1}{(\mu + 1)^2} \tilde{V}^\perp \tilde{V}^{\perp T} \right) RR^T \right]. \end{aligned}$$

The optimal μ that solves equation (5.2.1) can be found using the Newton iteration

$$\mu^{(t)} = \mu^{(t-1)} - \frac{f(\mu^{(t-1)}) - \tau}{\nabla f(\mu^{(t-1)})},$$

where $\nabla f(\mu)$ is given by

$$\begin{aligned} \text{Tr} \left[\left(\frac{-2\omega^4}{(\mu\omega^2 + 1)^2} \tilde{U} \tilde{U}^T + \frac{-2}{(\mu + 1)^3} \tilde{U}^\perp \tilde{U}^{\perp T} \right) LL^T \right. \\ \left. + \left(\frac{-2\omega^4}{(\mu\omega^2 + 1)^3} \tilde{V} \tilde{V}^T + \frac{-2}{(\mu + 1)^3} \tilde{V}^\perp \tilde{V}^{\perp T} \right) RR^T \right]. \end{aligned}$$

5.2.2 TRAVERSING THE PARETO CURVE

The design of an effective optimization method that solves (wBPDN $_{\sigma}$) requires 1) evaluating problem (5.1), and 2) computing the dual of the weighted nuclear norm $\|QXW\|_*$.

To compute the dual of the weighted nuclear norm, we follow Theorem 5.1 of Berg & Friedlander (2011) which defines the polar (or dual) representation of a weighted gauge function $\kappa(\Phi x)$ as $\kappa^o(\Phi^{-1}x)$, where Φ is an invertible linear operator. The weighted nuclear norm $\|QXW\|_*$ is in fact a gauge function with invertible linear weighting matrices Q and W . Therefore, the dual norm is given by

$$(\|Q(\cdot)W\|_*)_d(Z) := \|Q^{-1}ZW^{-1}\|_{\infty}.$$

6. Numerical experiments

We test the performance of our algorithm on two example applications. We first consider the Netflix problem, which is often solved using rank minimization Funk (2006); Gross (2011); Recht & Ré (2011), and use it to illustrate the advantages of regularization in general and of the (BPDN $_{\sigma}$) formulation in particular. We then apply the proposed methods and extensions to seismic trace interpolation, a key application in exploration geophysics Sacchi et al. (1998), where rank regularization approaches have recently been successfully used Oropeza & Sacchi (2011).

6.1 The Netflix problem

We tested the performance of our algorithm on the MovieLens (1M) dataset, which contains 1,000,209 anonymous ratings of approximately 3,900 movies made by 6,040 MovieLens users. The ratings are on an integer scale from 1 to 5. The ratings matrix is not complete, and the goal is to infer the values in the unseen test set. In order to test our algorithm, we further subsampled the available ratings by randomly removing 50% of the known entries. We then solved the (BPDN $_{\sigma}$) formulation to complete the matrix, and compared the predicted (P) and actual (A) removed entries in order to assess algorithm performance. We report the signal-to-noise ratio (SNR):

$$\text{SNR} = 20 \log \left(\frac{\|A\|}{\|P - A\|} \right)$$

for different values of σ in the (BPDN $_{\sigma}$) formulation.

Since our algorithm requires pre-defining the rank of the factors L and R , we perform the recovery with the rank $k \in \{5, 10, 30, 50\}$. Table 1 shows the reconstruction SNR for each of the ranks k and for a relative error $\sigma \in \{0.5, 0.3, 0.2\}$ (the data mismatch is reduced to a fraction σ of the initial error). The last row of table 1 shows the recovery for the unconstrained factorized formulation obtained using LSQR; this corresponds to $\sigma \approx 0$. It is clear that for small k , we get good results without regularization; however, as k increases, the quality of the LSQR results quickly decay. The best results are obtained by picking a reasonably high k and using regularization. This observation demonstrates the importance of the nuclear norm regularization, especially when the underlying rank of the problem is unknown.

Table 2 shows the value of $\|LR^T\|_*$ of the reconstructed signal corresponding to the settings in Table 1. While the σ values are straightforward, the nuclear norm to predict ahead of time for the (LASSO $_{\tau}$) formulation. The final values of $\|LR^T\|_*$ in table (2) are automatically found by the root finding algorithm to solve $v(\tau) = \sigma$, for the σ values in table 1.

	k	5	10	30	50
σ					
0.5		6.2	7	7.1	6.3
0.3		10.9	10.2	10.7	10.3
0.2		12.2	12.4	12.5	12.6
LSQR		12.2	11.3	8.7	7.8

Table 1: Summary of the recovery results (SNR in dB) on the Movielens (1M) data set for factor rank k and relative error level σ for (BPDN $_{\sigma}$). The last row gives recovery results for the non-regularized data fitting factorized formulation solved with LSQR. Quality *degrades* with k due to overfitting for the non-regularized formulation, and improves with k when regularization is used.

	k	5	10	30	50
σ					
0.5		6e3	7e3	7e3	6e3
0.3		1.1e4	1.0e4	1.1e4	1.0e4
0.2		2.5e5	0.8e5	0.8e5	0.8e5

Table 2: Nuclear-norms of the solutions LR^T for results in Table 1, corresponding to τ values in (LASSO $_{\tau}$). These values are found automatically via root finding, but are difficult to guess ahead of time.

6.2 Seismic missing-trace interpolation

In exploration seismology, extremely large amounts of data (often on the order of petabytes) must be acquired and processed in order to determine the structure of the subsurface. In many situations, only a subset of the complete data is acquired due to physical and/or budgetary constraints. Moreover, recent insights from the field of compressed sensing allow for deliberate subsampling of seismic wavefields in order to improve reconstruction quality and reduce acquisition costs Herrmann & Hennenfent (2008). The acquired subset of the complete data is often chosen by randomly subsampling a dense regular source or receiver grid. Interpolation algorithms are then used to reconstruct the dense regular grid in order to perform additional processing on the data such as removal of artifacts, improvement of spatial resolution, and key analysis, such as migration.

Seismic data is organized in *seismic lines*, where N_r receivers and N_s sources are collocated in a straight line. The sources are deployed sequentially and the receivers record each shot record for a period of N_t time samples. For our experiments, we apply our algorithm to interpolate a seismic line from the Gulf of Suez. The data contains $N_s = 354$ sources, $N_r = 354$ receivers, and $N_t = 1024$ with a sampling interval of 0.004s, leading to a shot duration of 4s and a maximum temporal frequency of 125 Hz. Most of the energy of the seismic line is preserved in the 12-60Hz frequency band. Figs. 1(a) and (b) illustrate the 12Hz and 60Hz frequency slices in the source-

receiver domain, respectively. In order to simulate missing traces, we apply a subsampling mask that randomly removes 50% of the sources, resulting in the subsampled frequency slices illustrated in Figs. 1 (c) and (d).

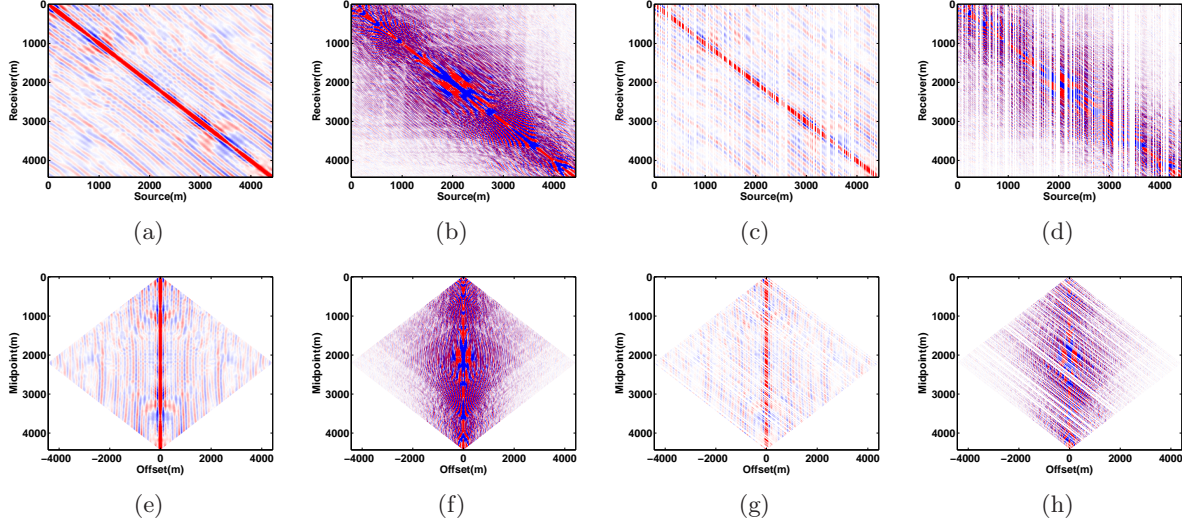


Figure 1: Frequency slices of a seismic line from Gulf of Suez with 354 shots, 354 receivers. Fully data for (a) low frequency at 12 Hz and (b) high frequency at 60 Hz in s-r domain. Subsampled data with $\delta = 0.5$ for (c) low frequency at 12 Hz and (d) high frequency at 60 Hz in s-r domain. Full data for (e) low frequency at 12 hz and (f) high frequency at 60 Hz in m-h domain. Subsampled data with $\delta = 0.5$ for (g) low frequency at 12 Hz and (h) high frequency at 60 Hz in m-h domain.

State of the art trace interpolation schemes transform the data into sparsifying domains, for example using the Fourier Sacchi et al. (1998) and Curvelet Herrmann & Hennenfent (2008) transforms. The underlying sparse structure of the data is then be exploited to recover the missing traces. However, seismic data also has matrix structure, and low-rank formulations can be used to design matrix-completion trace interpolation strategies.

The main challenge in applying rank-minimization for seismic trace interpolation is to find a transform domain that satisfies the following two properties:

1. fully sampled seismic lines have low-rank structure (quickly decaying singular values), and
2. subsampled seismic lines have high rank (slowly decaying singular values).

When these two properties hold, rank-penalization formulations allow the recovery of missing traces. In our experiments, we use the transformation from the source-receiver (s-r) domain to the midpoint-offset (m-h). The conversion from (s-r) domain to (m-h) domain is a coordinate transformation, with the midpoint is defined by $m = \frac{1}{2}(s + r)$ and the half-offset is defined by $h = \frac{1}{2}(s - r)$. This transformation is illustrated by transforming the 12Hz and 60Hz source-receiver domain frequency slices in Figs. 1(a) and (b) to the midpoint-offset domain frequency slices in

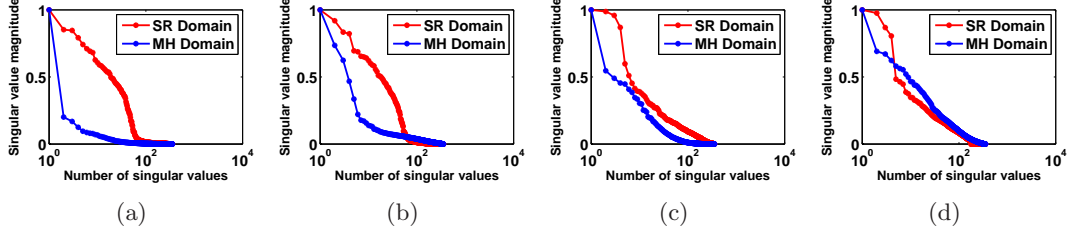


Figure 2: Singular value decay of fully sampled (a) low frequency slice at 12 Hz and (c) high frequency slice at 60 Hz in (s-r) and (m-h) domains. Singular value decay of 50% subsampled (b) low frequency slice at 12 Hz and (d) high frequency data at 60 Hz in (s-r) and (m-h) domains. Notice that decay of singular values is faster in midpoint-offset domain. Sub-sampling does not noticeably change the decay of singular value in (s-r) domain; but destroys fast decay of singular values in (m-h) domain.

Figs. 1(e) and (f). The corresponding subsampled frequency slices in the midpoint-offset domain are shown in Figs. 1(g) and (h).

To show that the midpoint-offset transformation achieves aims 1 and 2 above, we plot the decay of the singular values of both the 12Hz and 60Hz frequency slices in the source-receiver domain and in the midpoint-offset domain in Figs. 2 (a) and (c). Notice that the singular values of both frequency slices decay faster in the midpoint-offset domain, and that the singular value decay is slower for subsampled data in Figs. 2 (b) and (d).

Let \mathbf{X} denote the data matrix in the midpoint-offset domain and let \mathbf{R} be the subsampling operator that maps Figs. 1 (e) and (f) to Figs. 1(g) and (h). Denote by \mathcal{S} the transformation operator from the source-receiver domain to the midpoint-offset domain. The resulting measurement operator in the midpoint-offset domain is then given by $\mathcal{A} = \mathbf{R}\mathcal{S}^H$.

We formulate and solve the matrix completion problem (BPDN_σ) to recover the 12Hz and 60Hz frequency slices in the (m-h) domain. We limit the number of iterations to 300 and set the rank equal to 10 for the low frequency slice, and rank equal to 30 for the high frequency slice. Figures 3(a) and (b) show the recovery and error plot for the low frequency slice at 12 Hz, respectively. Figures 3(c) and (d) show the recovery and error plot for the high frequency slice at 60 Hz, respectively. The reconstruction error is smaller in the low frequency slice compared to the high frequency slice, which agrees with expectations since the low frequency data has lower rank than high frequency data.

In order to illustrate the importance of the nuclear-norm regularization, we solved the interpolation problem using a simple least-squares formulation on the same seismic data set. The least squares problem was solved using the L , R factorization structure, thereby implicitly enforcing a rank on the recovered estimate. The problem was then solved with the factors L and R having a rank $k \in \{5, 10, 20, 30, 40, 50, 80, 100\}$. The reconstruction SNRs comparing the recovery for the regularized and non-regularized formulations are shown in Fig. 4. The figure shows that the performance of the non-regularized approach decays with rank, due to overfitting. The regularized approach, in contrast, obtains better recovery as the factor rank increases.

6.2.1 RE-WEIGHTING

Re-weighting for seismic trace interpolation was recently used in Mansour et al. (2012) to improve the interpolation of subsampled seismic traces in the context of sparsity promotion in the curvelet domain. The weighted ℓ_1 formulation takes advantage of curvelet support overlap across adjacent frequency slices.

Analogously, in the matrix setting, we use the weighted rank-minimization formulation (wBPDN_σ) to take advantage of correlated row and column subspaces for adjacent frequency slices. We first demonstrate the effectiveness of solving the (wBPDN_σ) problem when we have accurate subspace information. For this purpose, we compute the row and column subspace bases of the fully sampled low frequency (11Hz) seismic slice and pass this information to (wBPDN_σ) using matrices Q and W . Figures 5(a) and (b) show the residual of the frequency slice with and without weighting. The reconstruction using the (wBPDN_σ) problem achieves a 1.5dB improvement in SNR over the non-weighted (BPDN_σ) formulation.

Next, we apply the (wBPDN_σ) formulation in a practical setting where we do not know subspace bases ahead of time, but learn them as we proceed from low to high frequencies. We use the row and column subspace vectors recovered using (BPDN_σ) for 10.75 Hz and 15.75 Hz frequency slices as subspace estimates for the adjacent higher frequency slices at 11 Hz and 16 Hz. Using the (wBPDN_σ) formulation in this way yields SNR improvements of 0.6dB and 1dB, respectively, over (BPDN_σ) alone. Figures 6(a) and (b) show the residual for the next higher frequency without using the support and Figures 6(c) and (d) shows the residual for next higher frequency with support from previous frequency. Figure 7 shows the recovery SNR versus frequency for weighted and non-weighted cases for a range of frequencies from 9 Hz to 17 Hz.

7. Conclusions

We have presented a new method for matrix completion. Our method combines the Pareto curve approach for optimizing (BPDN_σ) formulations with SVD-free matrix factorization methods. We demonstrated the advantages of the (BPDN_σ) formulation on the Netflix problem, and obtained high-quality reconstruction results for the seismic trace interpolation problem. We also proposed a weighted extension (wBPDN_σ), and used it to incorporate subspace information we learned on the fly to improve interpolation in adjacent frequencies.

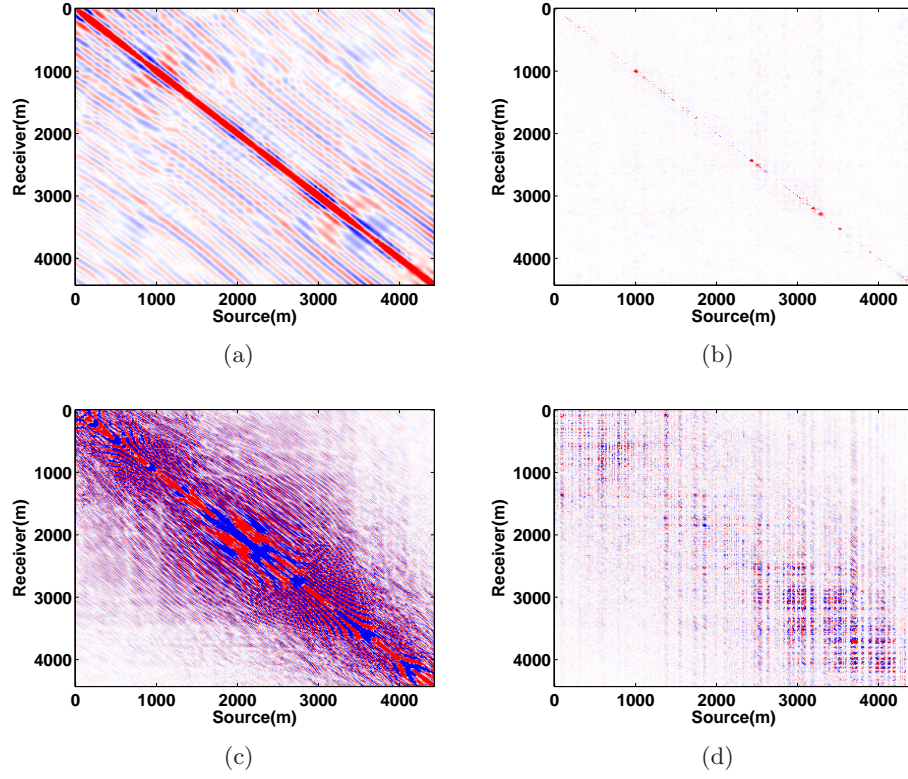


Figure 3: Recovery results for subsampled 2D frequency slices with $\delta = 0.5$ using the nuclear norm formulation. (a) Interpolation and (b) residual of low frequency slice at 12 Hz with SNR = 19.1 dB. (c) Interpolation and (d) residual of high frequency slice at 60 Hz with SNR = 15.2 dB.

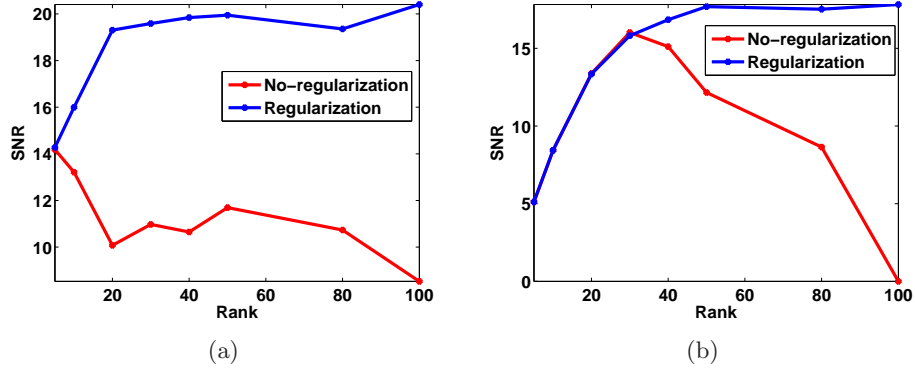


Figure 4: Comparison of regularized and non-regularized formulations. SNR of (a) low frequency slice at 12 Hz and (b) high frequency slice at 60 Hz over a range of factor ranks. Without regularization, recovery quality decays with factor rank due to over-fitting; the regularized formulation improves with higher factor rank.

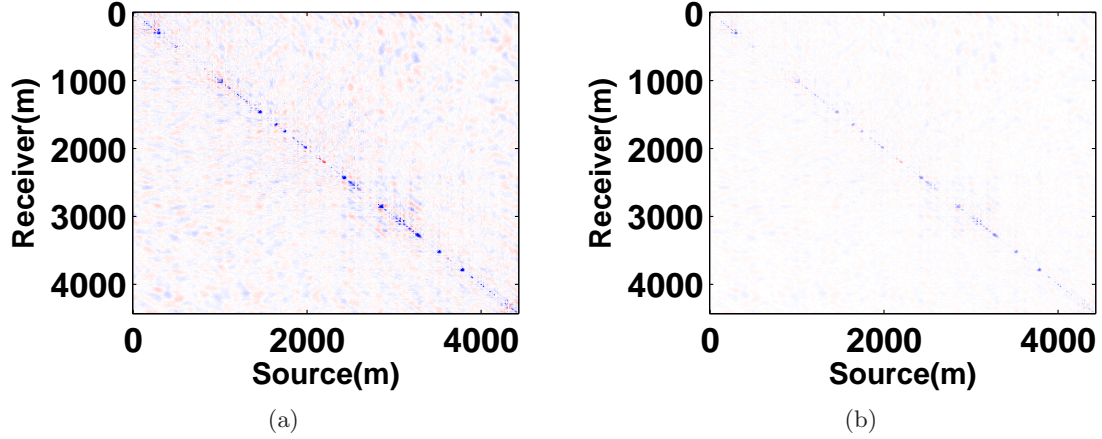


Figure 5: Residual error for recovery of 11 Hz slice (a) without weighting and (d) with weighting using true support. SNR in this case is improved by 1.5 dB.

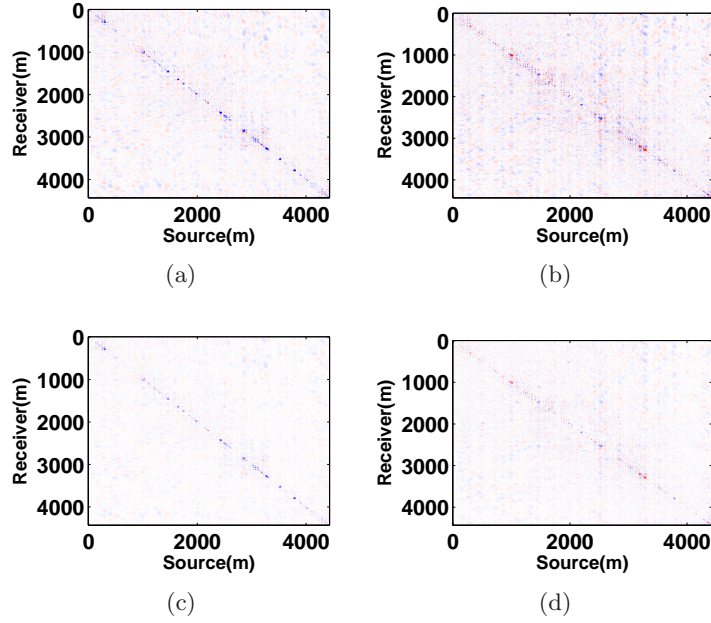


Figure 6: Residual of low frequency slice at 11 Hz (a) without weighing (c) with support from 10.75 Hz frequency slice. SNR is improved by 0.6 dB. Residual of low frequency slice at 16 Hz (b) without weighing (d) with support from 15.75 Hz frequency slice. SNR is improved by 1dB. Weighting using learned support is able to improve on the unweighted interpolation results.

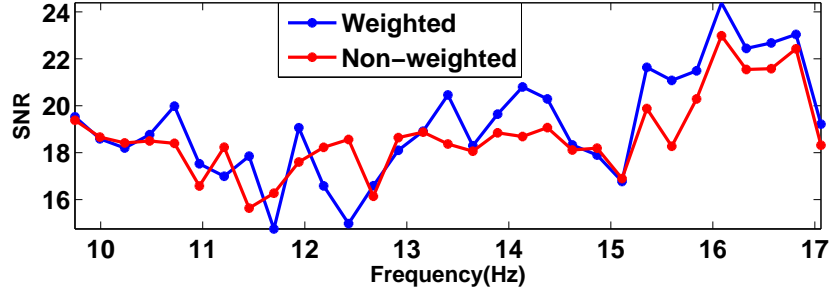


Figure 7: Recovery results of practical scenario in case of weighted factorized formulation over a frequency range of 9-17 Hz. The weighted formulation outperforms the non-weighted for higher frequencies. For some frequency slices, the performance of the non-weighted algorithm is better, because the weighted algorithm can be negatively affected when the subspaces are less correlated.

References

- Aravkin, A.Y., Burke, J.V., and Friedlander, M.P. Variational properties of value functions. *submitted to SIAM J. Opt.*, *arXiv:1211.3724*, 2012.
- Berg, E. van den and Friedlander, M. P. Probing the pareto frontier for basis pursuit solutions. *SIAM Journal on Scientific Computing*, 31(2):890–912, 2008.
- Berg, E. van den and Friedlander, M. P. Sparse optimization with least-squares constraints. *SIAM J. Optimization*, 21(4):1201–1229, 2011.
- Candès, E., Li, X., Ma, Y., and Wright, J. Robust principal component analysis? *Journal of the ACM*, 58(3), May 2011.
- Candès, E. J. and Tao, T. Near-optimal signal recovery from random projections: Universal encoding strategies. *Information Theory, IEEE Transactions on*, 52(12):5406–5425, dec. 2006.
- Donoho, D. Compressed sensing. *IEEE Transactions on Information Theory*, 52(4):1289–1306, 2006.
- Fazel, M. *Matrix rank minimization with applications*. PhD thesis, Stanford University, 2002.
- Figueiredo, M.A.T., Nowak, R.D., and Wright, S.J. Gradient projection for sparse reconstruction: Application to compressed sensing and other inverse problems. *IEEE Journal of Selected Topics in Signal Processing*, 1(4):586–597, dec. 2007.
- Friedlander, M., Mansour, H., Saab, R., and Yilmaz, O. Recovering compressively sampled signals using partial support information. *IEEE Transactions on Information Theory*, 58(1), January 2011.
- Funk, S. Netflix update: Try this at home, December 2006. URL <http://sifter.org/~simon/journal/20061211.html>.
- Gross, David. Recovering Low-Rank Matrices From Few Coefficients in Any Basis. *IEEE Transactions on Information Theory*, 57:1548–1566, 2011.
- Herrmann, F. J. and Hennenfent, G. Non-parametric seismic data recovery with curvelet frames. *Geophysical Journal International*, 173(1):233–248, 2008. ISSN 1365-246X.
- Lee, J., Recht, B., Salakhutdinov, R., Srebro, N., and Tropp, J. In *Advances in Neural Information Processing Systems, 2010*.
- Lee, J., Recht, B., Salakhutdinov, R., Srebro, N., and Tropp, J. Practical large-scale optimization for max-norm regularization. In Lafferty, J., Williams, C. K. I., Shawe-Taylor, J., Zemel, R.S., and Culotta, A. (eds.), *Advances in Neural Information Processing Systems 23*, pp. 1297–1305. 2010.
- Mairal, J., Elad, M., and Sapiro, G. Sparse representation for color image restoration. *IEEE Transactions on Image Processing*, 17(1):53–69, Jan. 2008.

- Mansour, H., Saab, R., Nasiopoulos, P., and Ward, R. Color image desaturation using sparse reconstruction. In *Proc. of the IEEE International Conference on Acoustics, Speech, and Signal Processing (ICASSP)*, pp. 778–781, March 2010.
- Mansour, H., Herrmann, F. J., and Yilmaz, O. Improved wavefield reconstruction from randomized sampling via weighted one-norm minimization. *submitted to Geophysics*, 2012.
- Neelamani, R., Krohn, C. E., Krebs, J. R., Romberg, J. K., Deffenbaugh, Max, and Anderson, John E. Efficient seismic forward modeling using simultaneous random sources and sparsity. *Geophysics*, 75(6):WB15–WB27, 2010.
- Oropeza, V. and Sacchi, M. Simultaneous seismic data denoising and reconstruction via multichannel singular spectrum analysis. *Geophysics*, 76(3):V25–V32, 2011.
- Recht, B. and Ré, C. Parallel stochastic gradient algorithms for large-scale matrix completion. In *Optimization Online*, 2011.
- Recht, B., Fazel, M., and Parrilo, P.A. Guaranteed minimum rank solutions to linear matrix equations via nuclear norm minimization. *SIAM Review*, 52(3):471–501, 2010.
- Rennie, J. D. M. and Srebro, N. In *ICML ’05 Proceedings of the 22nd international conference on Machine learning*.
- Sacchi, M.D., Ulrych, T.J., and Walker, C.J. Interpolation and extrapolation using a high-resolution discrete fourier transform. *Signal Processing, IEEE Transactions on*, 46(1):31–38, jan 1998.
- Starck, J.-L., Elad, M., and Donoho, D. Image decomposition via the combination of sparse representation and a variational approach. *IEEE Transaction on Image Processing*, 14(10), 2005.